Accuracy Evaluation of Human Gait Estimation by a Sparse Set of Inertial Measurement Units

Tsubasa Maruyama, Haruki Toda, Suguru Kanoga, Mitsunori Tada, and Yui Endo

Abstract Inertial measurement units (IMUs) have been utilized as motion-capture (MoCap) devices in computer graphics, biomechanics, and rehabilitation. Typically, full-body motions are estimated from the orientation and/or acceleration data of 13 to 17 IMUs attached to the body segments of experimental subjects. However, attaching numerous IMUs is quite intrusive and sometimes restricts the subjects' motions. Recent advances in machine learning technologies have enabled full body motion estimation from a sparse set of IMUs (6 to 7 units). The present study compares the motion estimation accuracies of a system with a full set of IMUs (called full IMU MoCap) and a system with a sparse set of IMUs (called sparse IMU MoCap). Three male subjects performed three walking trials with different stride lengths (normal, short, and long), and their full body motions were estimated by each MoCap. Finally, the gait-related factors were calculated from each set of motion estimation results, and compared with the ground-truth data obtained by an optical marker-based MoCap. Although the sparse IMU MoCap achieved a lower overall accuracy than the full IMU MoCap, it can potentially evaluate the relative changes in the functionality of the locomotor during walking.

1 Introduction

In computer graphics, biomechanics, and rehabilitation, full-body motions are often measured by motion capture (MoCap) based on inertial measurement units (IMUs) [1]. In such systems, a subject's motion is estimated from the orientation and/or acceleration data of different IMUs attached to different body segments. These measurements usually require 13 to 17 IMUs. IMU-based MoCap is not limited to laboratory environments, but can also be used onsite such as in clinic, care facility, outdoor, and daily-living environments [2].

Meanwhile, full body motion estimation using a sparse set of IMUs has been proposed for computer graphics research [3, 4]. For example, Mousas et al. attached

Tsubasa Maruyama, Haruki Toda, Suguru Kanoga, Mitsunori Tada, and Yui Endo

Artificial Intelligence Research Center, AIST, 2-3-26 Aomi, Koto-ku, Tokyo 135-0064, Japan,{tbs-maruyama, haruki-toda, s.kanouga, m.tada, y.endo}@aist.go.jp

a single IMU to the foot, and estimated the full body motion of the subject by a hierarchical multivariate hidden Markov model [3]. Huang et al. proposed a deep inertial poser (DIP) that enables full body motion estimation from the data of a sparse set of IMUs attached on the sacrum, wrists, lower legs, and head [4]. In this system, the full body motion is estimated by deep learning with training data obtained from the simulated IMU data. The averaged errors in the joint angle and joint position of this system were 17.54° and 64.9 mm, respectively. Although the IMU-based MoCap using a sparse set of IMUs (called *sparse IMU MoCap*) has lower motion estimation accuracy than the IMU-based MoCap using a full set of IMUs (called *full IMU MoCap*), it places less burden on the subjects' bodies. Attaching numerous IMUs is intrusive (especially for elderly subjects, motion-impaired patients, and industrial workers), and sometimes restricts the subject's motion. Sparse IMU MoCap is potentially suitable for activity recognition such as walking, standing, and object lifting in living or working environments, where high estimation accuracy of the joint angles is not always necessary.

Several studies have validated the full IMU MoCap in real-world situations [2, 5, 6]. Examples are gait analysis in a rehabilitation scenario by Teufl et al. [2] and Toda et al. [5], and stability of the center-of-mass and base-of-support movements by Guo et al. [6]. These studies have demonstrated the feasibility of the full IMU MoCap in biomechanics and rehabilitation applications. In general, gait analysis is done for revealing the environment-related human factors, gait diagnosis, evaluating the rehabilitation effect, and evaluating the effect of the walking assist device. However, attaching numerous IMUs is intrusive (especially for elderly subjects, patients with gait disorder), and sometimes restricts the subject's motion. On the other hand, the sparse IMU is less burden on the subjects' bodies, and the IMUs can be placed into the accessories such as belt, wrist watch, and shoes.

The present study aims to evaluate the motion estimation accuracy of sparse IMU MoCap in gait analysis. The gait-related factors calculated by sparse and full IMU MoCaps were compared with the ground-truth data obtained from a marker-based optical MoCap. A DIP [4] was employed as the sparse IMU MoCap, and our previously developed IMU MoCap [5,7,8] was employed as the full IMU MoCap.

2 Method

2.1 Overview

Fig. 1 is an overview of the present study. Prior to motion estimation (the scope of this paper), an individual digital human model (DHM) was constructed by Endo et al.'s method [9, 10] (Fig. 1 (A1)). In this method, all body dimensions are estimated from the subject's height and weight by principal component analysis using the Japanese body-size database [11]. Next, the full and sparse IMU MoCaps were subjected to inertial to segment (I2S) calibration, which calculates the IMU orientations relative to the body segments (Fig.1 (A2)) [8]. The same standing pose was employed for the I2S calibration of both systems. The full body motion was then estimated by both MoCap systems (Fig.1 (A3) and (A4)). Finally, the gait-related factors were calculated by both MoCap systems (Fig. 1 (A5)) and compared with the ground-truth measurements. Processes (A3)–(A5) are detailed in the following subsections.

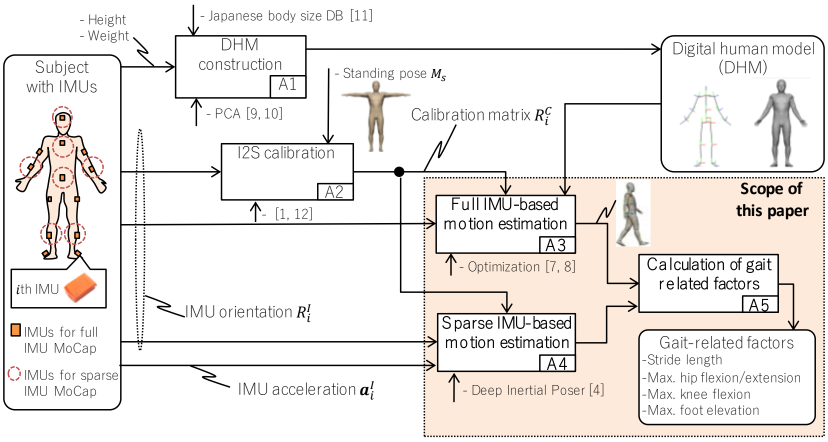

Fig. 1. Overview of the present study

2.2 Full IMU MoCap

Our previously developed system [7, 8] was employed as the full IMU MoCap. This system tracks the motions of the pelvis, sternum, head, upper arms, forearms, thighs, lower legs, and feet using the data of 13 IMUs. All joint angles of the DHM were estimated such that the segment orientation of the DHM fitted the orientation data of the corresponding IMU. As reported in the literature [12], the full IMU MoCap can estimate the pelvis transition from its initial position. However, in this study, the pelvis position was fixed to meet the motion estimation condition of the sparse IMU MoCap. Details and further applications of this system are described elsewhere [7, 12].

2.3 Sparse IMU MoCap

The DIP in [4] was employed as the sparse IMU MoCap. The DIP estimates all joint angles from the orientation and acceleration data of IMUs attached on the forearms, lower legs, pelvis, and head. The estimation was performed by a bidirectional recurrent neural network model trained on the TotalCapture [13] and DIP–IMU [4] datasets. As the TotalCapture dataset contains no IMU measurements, the IMU orientation and acceleration data were generated by the motion simulation, and were fine-tuned using the DIP–IMU dataset. In the original study [4], fine-tuning improved the motion estimation results, giving average estimation accuracies of 17.54° and 64.9 mm for the angles and positions of the joints, respectively. Here we employed the demonstration system including the pretrained model data available in [14].

2.4 Calculation of the Gait-related Factors

In a typical gait analysis [15], the peak value of the joint-angle profile of the legs is measured during one gait cycle. The present study focuses on the stride length d_s, the maximum hip-flexion angle $\max_{\varphi\in\phi}\theta_{hf}(\varphi)$, the maximum hip-extension angle $\max_{\varphi\in\phi}\theta_{he}(\varphi)$, the maximum knee-extension angle $\max_{\varphi\in\phi}\theta_{k}(\varphi)$, and the maximum foot elevation angle $\max_{\varphi\in\phi}\theta_{f}(\varphi)$, where $\phi \in [0,1]$ represents a normalized gait cycle (see Fig. 2). These gait-related factors (calculated at each step) are related to the locomotor function and fall prevention during walking.

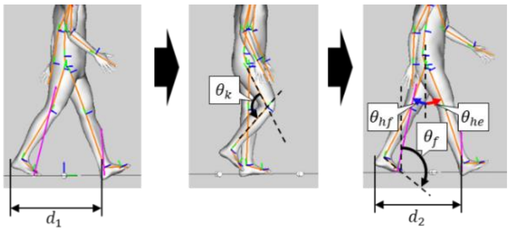

Fig. 2 Gait-related factors evaluated in this study

- Stride length: d_s

  As estimating the pelvis transition by the sparse IMU MoCap is infeasible, the stride length was approximated by $d_s = d_1 + d_2$, where d_1 and d_2 denote the horizontal distance between the heel points projected on the sagittal plane at the timings of the right and left heel contacts, respectively (Fig. 2). Although the heel-contact timing can be extracted from IMU data by a suitable method [16], it was here obtained by force-plate data for validation purposes.
- Maximum hip-flexion angle: $\max_{\varphi\in\phi}\theta_{hf}(\varphi)$

  $\theta_{hf}(\varphi)$ was calculated as the angle between the pelvis and the femur of the swing leg. In general, the maximum $\theta_{hf}(\varphi)$ relates to the foot displacements in the vertical and forward directions. When $\max_{\varphi\in\phi}\theta_{hf}(\varphi)$ is large, the fall risk is decreased and the stride length is increased.
- Maximum hip-extension angle: $\max_{\varphi\in\phi}\theta_{he}(\varphi)$

  $\theta_{hf}(\varphi)$ was calculated as the angle between the pelvis and the femur of the stance leg. Similarly to $\theta_{hf}(\varphi)$, the maximum $\theta_{he}(\varphi)$ relates to the body displacements in the vertical and forward directions. When $\max_{\varphi\in\phi}\theta_{he}(\varphi)$ is large, the locomotion is effective.

- Maximum knee-flexion angle: $\max_{\varphi \in \phi} \theta_k(\varphi)$

  $\theta_k(\varphi)$ was calculated as the angle between the femur and the tibia of the swing leg. The maximum $\theta_k(\varphi)$ relates to the toe clearance during walking. When $\max_{\varphi \in \phi} \theta_k(\varphi)$ is large, the motion of the swing leg reduces the fall risk.
- Maximum foot-elevation angle: $\max_{\varphi \in \phi} \theta_f(\varphi)$

  $\theta_f(\varphi)$ was calculated as the angle between the foot of the stance leg and the floor surface. As $\theta_f(\varphi)$ contributes to the locomotion during the latter phase of the stance phase, it relates to the stride of the gait.

All measurements, i.e., the data obtained by the marker-based optical MoCap, the full IMU MoCap, and the sparse IMU MoCap, were processed by the same calculation method for the gait-related factors.

3. Experiments

3.1 Experimental Setting

Three young male subjects participated in the study. To each subject, we attached 57 reflective markers for the marker-based optical MoCap and 13 IMUs (upper arms, forearms, upper legs, lower legs, feet, pelvis, chest, head) for both IMU MoCap systems. The marker-based MoCap was a Vicon system [17] with 15 IR cameras. The IMU was an Xsens MTw [18] identical to that used for collecting the DIP–IMU dataset for the sparse IMU MoCap.

3.2 Trials

Fig. 3 shows the motion measurement environment. Each subject performed 18 walking trials consisting of normal, short, and long strides over a series of force plates (6 trials each). The walking distance was 10 m in each trial. The walking steps were detected at the times of activation on each force plate. Steps that did not contact the force plates were excluded from the analysis. Consequently, 1–4 steps were obtained for the calculation of the gait-related factors from each walking trial.

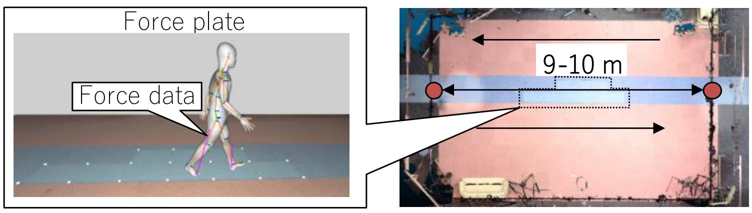

Fig. 3 Motion measurement environment

4. Results and Discussion

Fig. 4 compares the mean error in the stride length obtained by the two MoCap systems. The error was calculated as the difference between the ground-truth measurements and the estimates by the full or sparse IMU MoCap, and was averaged over all steps.

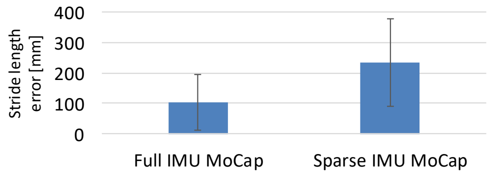

Fig. 4. Comparison of stride-length estimation errors. Error bars are the standard deviations.

Fig. 5 shows the results of the line fit method (LFM) [19]. When the estimates exactly agree with the measurements, the LFM result is $y = 1.0x + 0.0$. The R^2 values, representing the coefficients of determination, are defined as *very strong* ($R^2 \geq 0.64$), *strong* ($0.36 \leq R^2 < 0.64$), *moderately strong* ($0.16 \leq R^2 < 0.36$), *weak* ($0.04 \leq R^2 < 0.16$), or *very weak* ($R^2 < 0.04$). The sparse IMU MoCap was moderately strong correlated with the ground-truth (R^2 =0.24; see Fig. 5(b)), although the proportionality coefficient (i.e., the slope) was not close to 1.0.

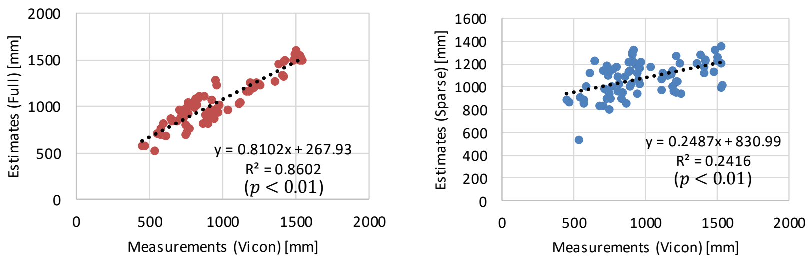

(a) Stride length of full IMU MoCap

(b) Stride length of sparse IMU MoCap

Fig. 5. Relations between stride length estimates and ground-truth measurements

Fig. 6 shows the mean joint-angle estimation errors between the ground-truth data and the full and sparse IMU MoCaps. The errors of both IMU MoCap systems were similar for the hip flexion and foot elevation, but the sparse IMU MoCap gave considerably larger errors in the hip extension and knee flexion than the full IMU MoCap.

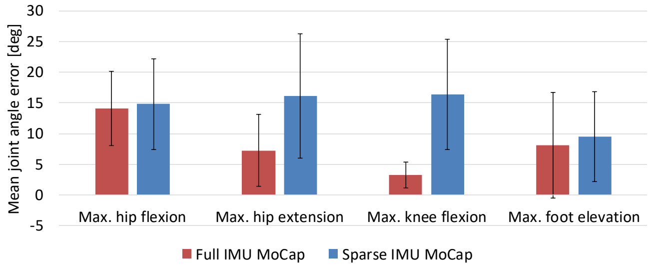

Fig. 6. Comparison of estimation errors in stride length between the full and sparse IMU MoCap

Fig. 7 shows the LFM results of the joint angle estimates, and Fig. 8 summarizes the coefficients of determination and proportionality obtained by LFM. The measurements of the sparse IMU MoCap were moderately strongly correlated with the ground-truths of the stride length ($R^2 = 0.24$) and the maximum knee flexion ($R^2 = 0.27$). In addition, strong correlations were confirmed for the maximum hip extension ($R^2 = 0.39$), maximum hip flexion ($R^2 = 0.61$) and maximum foot elevation ($R^2 = 0.54$). However, the proportionality coefficients were less than 0.7 without the maximum knee flexion and the foot elevation in the sparse IMU MoCap.

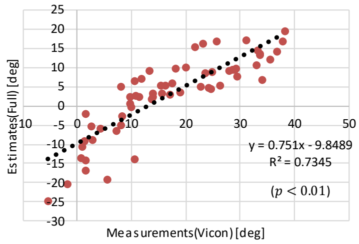

(a) $\max_{\varphi \in \phi} \theta_{hf}(\varphi)$ of full IMU MoCap

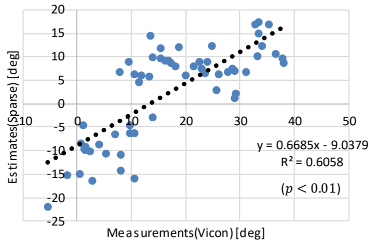

(b) $\max_{\varphi \in \phi} \theta_{hf}(\varphi)$ of sparse IMU MoCap

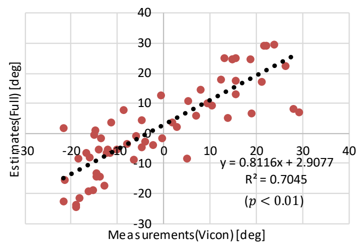

(c) $\max_{\varphi \in \phi} \theta_{he}(\varphi)$ of full IMU MoCap

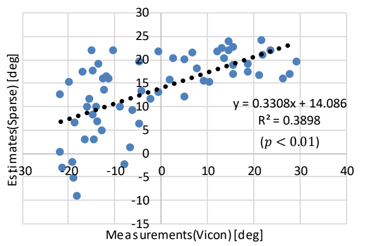

(d) $\max_{\varphi \in \phi} \theta_{he}(\varphi)$ of sparse IMU MoCap

Fig. 7 Relations between the joint-angle (hip flexion and hip extension) estimates of the MoCap systems and the ground-truth measurements

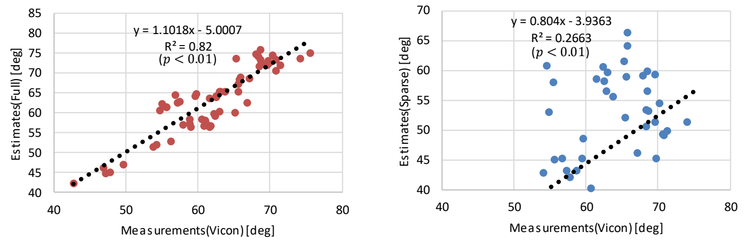

(e) $\max_{\varphi \in \phi} \theta_k(\varphi)$ of full IMU MoCap (f) $\max_{\varphi \in \phi} \theta_k(\varphi)$ of sparse IMU MoCap

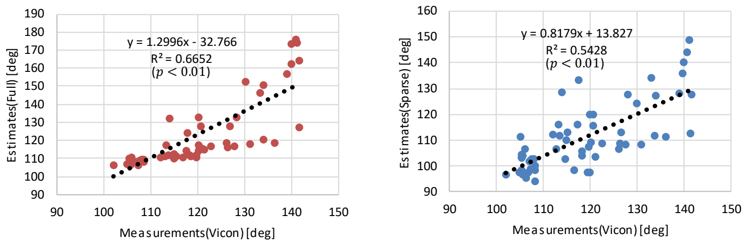

(g) $\max_{\varphi \in \phi} \theta_f(\varphi)$ of full IMU MoCap (h) $\max_{\varphi \in \phi} \theta_f(\varphi)$ of sparse IMU MoCap

Fig. 7 (cont.) Relations between the joint angle (knee flexion and foot elevation) estimates of the MoCap systems and the ground-truth measurements

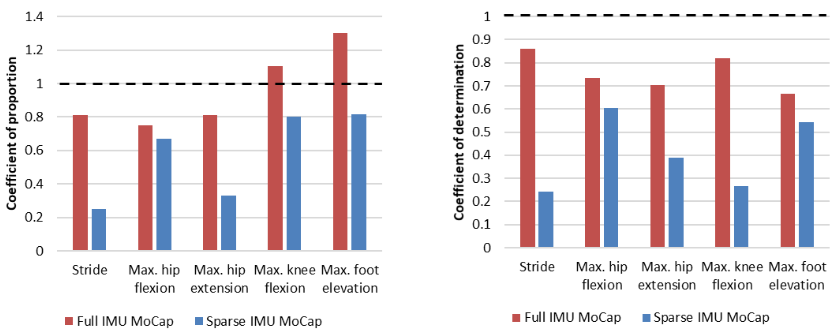

Fig. 8 Comparison of coefficients of proportionality (left) and determination (right) between full and sparse IMU MoCap

As already demonstrated in Figs. 4 and 6, the mean errors were larger in the sparse IMU MoCap than in the full IMU MoCap. This tendency is reasonable, because the sparse IMU MoCap installs fewer IMUs for the motion estimation than the full IMU MoCap. In addition, the proportionality coefficients of the sparse IMU MoCap were not always close to 1.0 (Fig. 8). This indicates that the sparse IMU MoCap cannot identify the absolute values of the gait-related factors.

On the other hand, strong correlations were confirmed for the maximum hip flexion (R^2 =0.61) and the maximum foot elevation (R^2 =0.54), indicating that both factors are related to the locomotor function of the subjects. Therefore, the sparse IMU MoCap can feasibly analyze the relative changes in the locomotor function of a subject's gait. For example, the sparse IMU MoCap can be utilized for evaluating the effect of the walking assist device by measuring the relative changes in the locomotor function [15]. Thus, the sparse IMU MoCap enables the gait analysis that is less burden for the subject than the full IMU MoCap in clinic, care facility, and outdoor environment [2, 5, 15].

As reported in the original literature [4], the estimation accuracy of IMU MoCap depends on the variation and amount of the training dataset. The accuracy is expected to be improved by measuring abnormal walking data (e.g., short and long stride lengths). However, measuring the motions of various subjects, including elderly subjects, is a difficult task. In gait analysis, the sparse IMU MoCap might be applicable to hip flexion and foot elevation, which can be reasonably reliably estimated by this method.

5. Conclusion

This study compared the motion estimation accuracies of the full and sparse IMU MoCap systems in gait analysis. Five gait-related factors (stride length, maximum hip-flexion and hip-extension angles, maximum knee-flexion angle, and maximum foot elevation angle) were evaluated. The accuracy of the gait factors depended on the number of IMUs used for the motion estimation, being lower in the sparse IMU MoCap than in the full IMU MoCap. However, the sparse IMU MoCap estimates were strongly correlated with the measured hip flexion and foot elevation, suggesting that sparse IMU MoCap is applicable to gait analysis and rehabilitation research. For example, sparse IMU MoCap might evaluate the effect of a walking assistive device based on the changes in the locomotion performance in indoor and outdoor environments.

Considering the difficulty of measuring abnormal walking motions, increasing the number of training data is not always a reasonable approach to improve the estimation accuracy of gait analysis. Recent proposals using a foot-mounted IMU [16, 20] can estimate the stride and minimum toe clearance, but measuring the hip and knee flexion angles is more problematic. Our future work will be addressed to develop a novel motion estimation system combining the machine learning-based approach (the sparse IMU MoCap) in foot movement estimation. With such improvements, we could determine the locomotion performance from several gait-related factors in the gait analysis and rehabilitation research fields.

Acknowledgments

This work was supported by JSPS KAKENHI Grant Number 19K15255.

References

[1] Roetenberg, D., Luinge H., Slycke, P.: Xsens MVN full 6DOF human motion tracking using miniature inertial sensors, Xsens Motion Technologies BV. Technical Report, 1-10, (2009)

[2] Teufl, W., Miezal, M., Taetzl, B., Fröhlich M., Bleser G.: Validity, test-retest reliability and long-term stability of magnetometer free inertial sensor based 3D joint kinematics, Journal of Sensors, **18** (7), 1980:1-1980:22, (2018)

[3] Mousas, C.: Full body locomotion reconstruction of virtual characters using a single inertial measurement unit, Journal of Sensors, **17**(11), 2589, (2017)

[4] Huang, Y., Kaufmann M., Aksan, E. Black, M. J., Hilliges, O., Pons-Moll, G.: Deep Inertial Poser: learning to reconstruct human pose from sparse inertial measurements in real time, ACM Trans. Graph. **37** (6), 185:1-185:15, (2018)

[5] Toda, H., Maruyama, T., Tada, M.: Validity of the kinematic profiles obtained by a real-time motion capture system using inertial measurement units during timed up and go test, 13th World Congress of International Society of Physical and Rehabilitation Medicine, (2019)

[6] Guo, L., Xiong, S.: Accuracy of base of support using an inertial sensor based motion capture system, Journal of Sensors, **17** (9), 2091:1-2091:24, (2007).

[7] Maruyama, T., Tada, M., Toda, H.: Riding motion capture system using inertial measurement units with contact constraints, Journal of Automation Technology, **13** (5), 506-516, (2019)

[8] Maruyama, T., Toda, H., Tada, M.: Inertial measurement unit to segment calibration based on constrained pose estimation, Proc. of SICE Annual Conference 2019, 719-722, (2019)

[9] Endo, Y., Tada, M., Mochimaru, M.: Dhaiba: development of virtual ergonomic assessment system with human models, Proc. of Digital Human Modeling 2014, #58, (2014)

[10] Endo, Y., Tada, M., Mochimaru, M.: Estimation of arbitrary human models from anthropometric dimensions, Proc. of the 17th International Conference on Human-Computer Interaction, 3-14, (2015)

[11] AIST Japanese Body Size Database, Available via https://unit.aist.go.jp/hiri/dhrg/ja/dhdb/91-92/index.html (In Japanese). Cited 30 Jan. 2020

[12] Maruyama, T., Tada, M., Sawatome, A., Endo, Y. Constraint-based real-time full body motion-capture using inertial measurement units, Proc. of 2018 IEEE International Conference on Systems, Man, and Cybernetics, 4298-4303, (2018)

[13] Trumble, M., Gilbert, A., Malleson, C., Hilton, A., Collomosse, J.: Total capture: 3d human pose estimation fusing video and inertial, Proc. of 28th British Machine Vision Conference, 1–13, (2017)

[14] MPI DIP, Available via http://dip.is.tuebingen.mpg.de/. Cited 30 Jan. 2020

[15] Toda, H., Tada, M., Maruyama, T., Kurita, Y.: Effect of contraction parameters on swing support during walking using wireless pneumatic artificial muscle driver: a preliminary study, Proc. of SICE Annual Conference 2019, 727-732, (2019)

[16] Kanzaki, T., Sawatome A., Tsuichihara S., Takemura H., Tada M.: Increasing exercise intensity during walking by sound intervention using real-time gait event detection, Proc. of the 2019 IEEE/SICE International Symposium on System Integration, 681-686, (2020)

[17] Vicon, Available in https://www.vicon.com/. Cited 30 Jan. 2020

[18] Xsens MTw Awinda, Available in https://www.xsens.com/products/mtw-awinda/. Cited 30 Jan. 2020

[19] Iosa, M., Cereatti, A., Merlo, A., Campanini, I., Paolucci, S., Cappozzo, A.: Assessment of waveform similarity in clinical gait data: the linear fit method. Journal of Biomedicine and Biotechnology, 2014, 214156:1-214156:7, (2014)

[20] Ojeda, L. V., Zaferiou, A. M., Cain, S. M.: Estimating Stair running performance using inertial sensors, Journal of Sensors, **17** (11) 2647:1-2647:1, (2017)